

Sterile Neutrinos and Flavor Ratios in IceCube

Vedran Brdar,^a Joachim Kopp,^b and Xiao-Ping Wang^c

*PRISMA Cluster of Excellence and Mainz Institute for Theoretical Physics,
Johannes Gutenberg-Universität Mainz, 55099 Mainz, Germany*

The flavor composition of astrophysical neutrinos observed in neutrino telescopes is a powerful discriminator between different astrophysical neutrino production mechanisms and can also teach us about the particle physics properties of neutrinos. In this paper, we investigate how the possible existence of light sterile neutrinos can affect these flavor ratios. We consider two scenarios: (i) neutrino production in conventional astrophysical sources, followed by partial oscillation into sterile states; (ii) neutrinos from dark matter decay with a primary flavor composition enhanced in tau neutrinos or sterile neutrinos. Throughout the paper, we constrain the sterile neutrino mixing parameters from a full global fit to short and long baseline data. We present our results in the form of flavor triangles and, for scenario (ii), as exclusion limits on the dark matter mass and lifetime, derived from a fit to IceCube high energy starting events and through-going muons. We argue that identifying a possible flux of neutrinos from dark matter decay may require analyzing the flavor composition as a function of neutrino energy.

I. INTRODUCTION

In the era of multi-messenger astronomy, it is fair to say that we can not only see the Universe (using telescopes that cover the entire electromagnetic spectrum), but also hear the Universe (using gravitational wave detectors [1]), and taste the Universe (using neutrino telescopes). Regarding the latter, we are of course referring to the possibility of measuring the flavor of high-energy neutrinos and of using this information to learn about the properties of astrophysical neutrino sources and about the properties of neutrinos themselves. Indeed, the non-trivial information offered by the flavor ratios of astrophysical neutrino fluxes has been studied ever since the discovery of neutrino oscillations [2–13], and the topic has received a tremendous further boost in 2013 [14–31], thanks to the discovery of a high energy astrophysical neutrino flux by the IceCube collaboration [20, 25, 32, 33].

In this paper, we discuss in particular how the flavor ratios of ultra-high energy astrophysical neutrinos are affected in the presence of sterile neutrinos that have sizeable mixing with active neutrinos. Motivation for such scenarios comes for instance from the long-standing anomalies observed by some short-baseline oscillation experiments, in particular LSND [34], MiniBooNE [35], SAGE and GALEX [36, 37], as well as several reactor neutrino experiments [38–40] (see also [41–43]). Even though these results appear to be in some tension with non-observations in other experiments [44–51], they have motivated a multifarious experimental program aimed at testing them [52]. Compared to previous analyses studying high-energy astrophysical neutrino fluxes and flavor ratios in the presence of sterile states [3, 12, 14, 53, 54], we will comprehensively include constraints from short baseline oscillation experiments. We will achieve this by using the numerical fitting codes underlying the global fit from ref. [47]. Moreover, we will include the possibility that the initial flux of high-energy neutrinos is dominated by tau neutrinos or sterile neutrinos in some part of the energy spectrum. This can happen for instance in scenarios where PeV-scale dark matter (DM) particles decay to high energy active or sterile neutrinos. The latter scenario is particularly

^a vbrdar@uni-mainz.de

^b jkopp@uni-mainz.de

^c xiaowang@uni-mainz.de

interesting because the observed flavor ratios would depend mainly on the active–sterile mixing angles.

The outline of the paper is as follows: in section II we will collect the relevant analytic formulas for computing flavor ratios of high-energy neutrinos, and we will describe how we implement the constraints from oscillation experiments in our analysis. In section III, we will then present our results for the case of astrophysical neutrino sources and for a primary flux dominated by tau neutrinos or sterile neutrinos. We will show the accessible regions in the “flavor triangle” — the well-known ternary plot illustrating the fractions of electron, muon and tau neutrinos relative to the total flux of active neutrinos. In section IV we will discuss two toy models for heavy DM particles decaying to active or sterile neutrinos. These models serve as illustrative examples for scenarios with non-standard initial flavor composition. We will also constrain the parameter space of our toy models by fitting the HESE (high energy starting event) and TGM (through-going muon) data from IceCube. In section V, we summarize and conclude.

II. COMPUTING FLAVOR RATIOS IN THE PRESENCE OF STERILE NEUTRINOS

In the following, we discuss the production, propagation, and detection of high energy astrophysical neutrinos in the presence of an additional eV scale sterile neutrino ν_s that is a singlet under the $SU(3)_c \times SU(2)_L \times U(1)_Y$ gauge group of the Standard Model (SM). High energy astrophysical neutrinos are usually assumed to be produced in the decays of high energy pions, which in turn originate in collisions of high energy cosmic protons with other nucleons or with photons. The ensuing flavor composition of the primary flux is then $(\Phi_{\nu_e} : \Phi_{\nu_\mu} : \Phi_{\nu_\tau} : \Phi_{\nu_s}) \sim (1 : 2 : 0 : 0)$, unless muons rapidly lose energy before decaying, in which case the flavor composition of high energy neutrinos changes to $(\Phi_{\nu_e} : \Phi_{\nu_\mu} : \Phi_{\nu_\tau} : \Phi_{\nu_s}) \sim (0 : 1 : 0 : 0)$ [55–58]. Here, Φ_{ν_α} is the initial flux of neutrinos of flavor α . Alternative scenarios include neutrino production in neutron decay with initial flavor composition $(1 : 0 : 0 : 0)$ [5], or in decays of charm mesons, leading to a flavor composition of $(1 : 1 : 0 : 0)$ [10]. In the literature, an initial flavor ratio of $(0 : 0 : 1 : 0)$ is also studied for completeness [23], despite the lack of a plausible astrophysical production scenario. In this work we will study a simple model for PeV dark matter decaying dominantly to the third lepton generation. We will also consider the possibility that part of the astrophysical neutrino flux is initially sterile, i.e. has flavor composition $(0 : 0 : 0 : 1)$. Such a flux could originate, for instance, from dark matter decay into sterile neutrinos or from a dark sector with complex dynamics of its own, admitting the existence of “dark astrophysical accelerators” [59, 60].

Neutrinos are initially created as flavor eigenstates, i.e. coherent superpositions of mass eigenstates, that begin to oscillate as they propagate through space. However, as the distance from a typical astrophysical neutrino source is much larger than the coherence length, only the averaged effect of these oscillations is observable at Earth. Oscillation probabilities can thus be computed by treating the initial flux as an incoherent superposition of mass eigenstates. This approach is further justified by the fact that different neutrino mass eigenstates propagate at slightly different group velocities. By the time a neutrino arrives at Earth, its different mass eigenstate components are therefore separated in space and time and can no longer be detected coherently. With these considerations in mind, the flavor conversion probabilities for high energy neutrinos in a world with n (active + sterile) neutrino flavors are [61]

$$P_{\nu_\alpha \rightarrow \nu_\beta} = P_{\nu_\beta \rightarrow \nu_\alpha} = \delta_{\alpha\beta} - 2 \sum_{k>j} \text{Re}[U_{\alpha k}^* U_{\beta k} U_{\alpha j} U_{\beta j}^*] = \sum_{j=1}^n |U_{\alpha j}|^2 |U_{\beta j}|^2, \quad (1)$$

where U is the $n \times n$ leptonic mixing matrix. In this work we focus on the case $n = 4$ and adopt

the parameterization [47, 62]

$$U = R^{34}(\theta_{34})\tilde{R}^{24}(\theta_{24}, \delta_2)R^{23}(\theta_{23})R^{14}(\theta_{14})\tilde{R}^{13}(\theta_{13}, \delta_0)\tilde{R}^{12}(\theta_{12}, \delta_1), \quad (2)$$

where $R^{ij}(\theta_{ij})$ is a rotation matrix in the ij plane and $\tilde{R}^{ij}(\theta_{ij}, \delta_k)$ is a rotation matrix supplemented with an additional phase factor δ_k . Each of these matrices is unitary, which implies that their product U is unitary as well. In the 3+1 model (three active neutrinos and one sterile neutrino) considered here, there are six mixing angles θ_{ij} and three physical phases. (Majorana phases are omitted as they are not observable in oscillation experiments.)

In general, we have the following 12 parameters to consider

$$\Theta \equiv (\theta_{12}, \theta_{13}, \theta_{23}, \delta_0, \theta_{14}, \theta_{24}, \theta_{34}, \delta_1, \delta_2, \Delta m_{21}^2, \Delta m_{31}^2, \Delta m_{41}^2). \quad (3)$$

As $\Delta m_{21}^2, \Delta m_{31}^2$ are well measured and not related to a rotation matrix, we fix them at $|\Delta m_{21}^2| = 7.5 \times 10^{-5} \text{eV}^2$ and $|\Delta m_{31}^2| = 2.4 \times 10^{-3} \text{eV}^2$. In order to explore the viable parameter space for neutrino oscillations, we randomly generate 10^7 parameter sets Θ .

For each parameter set, we randomly draw Δm_{41}^2 between 0.1 eV² and 10 eV². As for the mixing angles and phases, we take them to be distributed according to the Haar measure [63–65], which reads in the four flavor case

$$d\Theta = d(\sin^2 \theta_{12}) d(\sin^2 \theta_{23}) d(\cos^4 \theta_{13}) d(\cos^6 \theta_{14}) d(\cos^4 \theta_{24}) d(\sin^2 \theta_{34}) d\delta d\delta_1 d\delta_2. \quad (4)$$

In other words, the distributions of $\sin^2 \theta_{12}$, $\sin^2 \theta_{23}$, $\cos^4 \theta_{13}$, etc., are flat. By generating parameter points according to the Haar measure, we ensure that our prior distribution is independent of the chosen parameterization of the mixing matrix [63]. Already when generating parameter points, we restrict the three standard mixing angles θ_{12} , θ_{23} , θ_{13} to their experimentally allowed 3σ ranges based on a three-flavor fit using the global fitting code from ref. [47]. Afterward, we process all generated points with the same code, but including sterile neutrinos. Our code includes the experimental data sets listed in table I. This allows us to assign a global χ^2 value to each parameter point.

We then use Bayesian statistics to determine the credible intervals for the parameters (see for instance ref. [66]). For each parameter set Θ , the probability of obtaining the observed data is given by

$$P(\text{data}|\Theta) = \exp \left[-\frac{\chi^2(\Theta)}{2} \right]. \quad (5)$$

The unconditional probability $P(\text{data}) = \int d\Theta P(\Theta) P(\text{data}|\Theta)$ in our case is obtained by integrating $P(\text{data}|\Theta)$ over all parameter sets. We choose a flat prior, $P(\Theta) = \text{const.}$, in accordance with our assumption that parameter sets have a flat distribution in the Haar measure. We now apply Bayes' theorem [66]

$$P(\Theta|\text{data}) = \frac{P(\text{data}|\Theta) P(\Theta)}{P(\text{data})} \quad (6)$$

to obtain the posterior probability $P(\Theta|\text{data})$ of a given parameter set Θ , given the data. The $\alpha\%$ credible region in parameter space is then obtained by ordering the parameter points in descending order in the posterior probability: $P(\Theta_1|\text{data}) > P(\Theta_2|\text{data}) > P(\Theta_3|\text{data}) > \dots$. We then choose an i_{max} such that

$$\sum_{i=1}^{i_{\text{max}}} P(\Theta_i|\text{data}) = \frac{\alpha}{100}. \quad (7)$$

All parameter points Θ_i with $i < i_{\text{max}}$ are included in the $\alpha\%$ credible interval, all other points are excluded.

Experiment	Oscillation channel(s)
Short and long-baseline reactors	$\bar{\nu}_e \rightarrow \bar{\nu}_e$
KAMLAND	$\bar{\nu}_e \rightarrow \bar{\nu}_e$
Gallium	$\nu_e \rightarrow \nu_e$
Solar neutrinos	$\nu_e \rightarrow \nu_e$, neutral current (NC) data
LSND/KARMEN ^{12}C	$\nu_e \rightarrow \nu_e$
CDHS	$\nu_\mu \rightarrow \nu_\mu$
MiniBooNE	$\bar{\nu}_\mu \rightarrow \bar{\nu}_e, \bar{\nu}_\mu \rightarrow \bar{\nu}_\mu$
MINOS	$\nu_\mu \rightarrow \nu_\mu$, NC data
Atmospheric neutrinos	$\bar{\nu}_\mu \rightarrow \bar{\nu}_\mu$
LSND	$\bar{\nu}_\mu \rightarrow \bar{\nu}_e$
KARMEN	$\bar{\nu}_\mu \rightarrow \bar{\nu}_e$
NOMAD	$\nu_\mu \rightarrow \nu_e$
E776	$\bar{\nu}_\mu \rightarrow \bar{\nu}_e$
Icarus	$\nu_\mu \rightarrow \nu_e$

TABLE I. Oscillation experiments used in our analysis, based on the global fit from ref. [47]. The column labeled “Oscillation channel(s)” indicates whether a given experiment is measuring disappearance or appearance of (anti)neutrinos.

III. PREDICTED NEUTRINO FLAVOR RATIOS

A useful tool in studying neutrino flavor ratios is a ternary diagram (“flavor triangle”) as shown in fig. 1 (a). The three axes correspond to the fraction of neutrinos detected as ν_e , ν_μ , and ν_τ , respectively. The predicted flavor ratios at Earth in the absence of sterile neutrinos are shown as colored regions in fig. 1 for different assumptions on the composition of the primary flux. These regions correspond to 95 % credible interval. In obtaining these credibility regions, we have followed the approach described in section II, based on the global fit from ref. [47], but we show for comparison also the preferred regions based on the more recent results from ref. [67] (dashed black contours) and ref. [68] (dashed gray contours). To obtain the latter, we assume the likelihood distributions for $\sin^2 \theta_{12}$, $\sin^2 \theta_{13}$, and $\sin^2 \theta_{23}$ to be Gaussian, with central values and widths taken from ref. [67, 68]. For the phase δ_0 , we assume a flat distribution in the interval $[-\pi, \pi]$. Note that we show only results assuming a normal mass hierarchy (NH) here. We have checked that the plot changes very little for the inverted hierarchy case. We also note good agreement between our results and those of refs. [23, 24]. Comparing the colored region in fig. 1 (a) to the 68% and 95% CL exclusion regions provided by IceCube (black contours) [69], we observe that only a neutron decay source with initial flavor composition (1 : 0 : 0) is in some tension with the data.

In fig. 1 (b), we illustrate in more detail how the flavor composition of astrophysical neutrinos at Earth in the standard 3-flavor scenario varies with the initial composition, which we assume here to be of the form $(\frac{x}{3} : 1 - \frac{x}{3} : 0)$. Varying x between 0 and 1 thus interpolates between the (0 : 1 : 0) and (1 : 2 : 0) flavor compositions. The observable dispersion in the flavor composition is again due to uncertainties in the measured standard mixing parameters.

Coming to the impact of sterile neutrinos on the flavor composition of astrophysical neutrinos, we show in fig. 2 the reachable parts of the flavor triangle including oscillations into sterile neutrinos. The oscillation parameters are constrained to lie in the 68% (left), 90% (middle), or 95% (right)

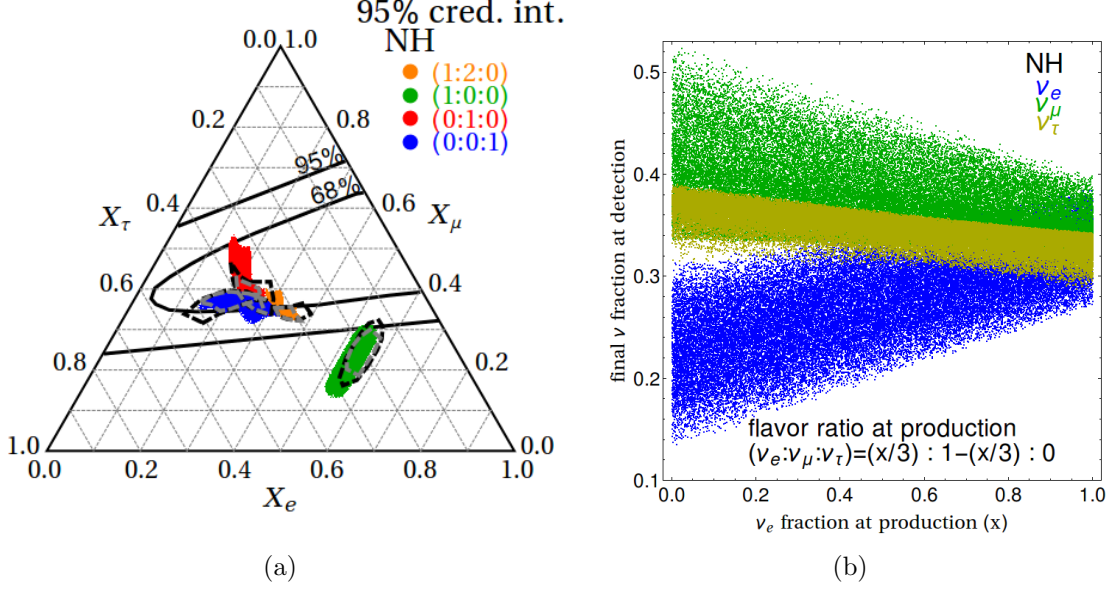


FIG. 1. (a) Flavor composition of high-energy astrophysical neutrinos at Earth for different assumptions on the initial flavor composition $\Phi_{\nu_e}^{\text{in}} : \Phi_{\nu_\mu}^{\text{in}} : \Phi_{\nu_\tau}^{\text{in}}$, assuming only standard three-flavor oscillations. The size of the colored regions represents the uncertainty in the three-flavor oscillation parameters based on the global fit developed in ref. [47]. For comparison, we also show results based on the more recent fits from ref. [67] (black dashed contours) and ref. [68] (gray dashed contours). Black solid contours indicate the flavor ratios preferred by IceCube data at the 68% and 95% confidence level [69]. Note that we show only results for normal neutrino mass ordering (NH) since the plot for inverted ordering would be almost identical. (b) Variation of the fractional ν_e , ν_μ and ν_τ fluxes at Earth as a function of the initial ν_e fraction x , assuming an initial flavor composition of the form $(\frac{x}{3} : 1 - \frac{x}{3} : 0)$.

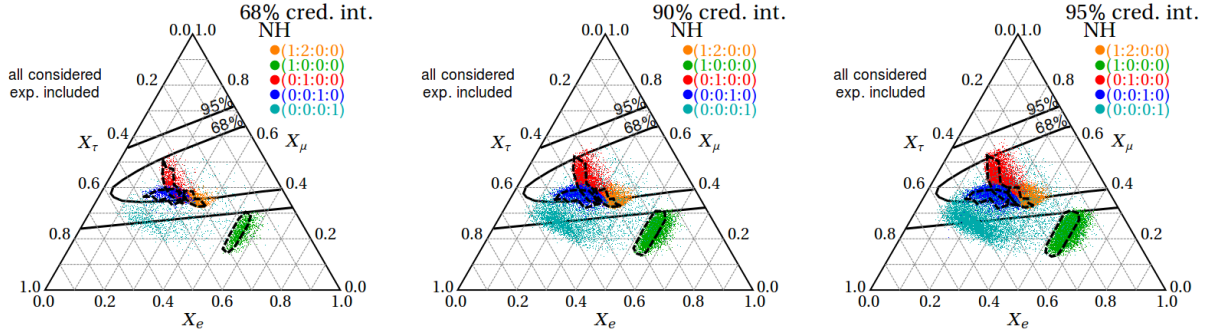


FIG. 2. Flavor composition of high-energy astrophysical neutrinos at Earth in the presence of sterile neutrinos. For the initial flavor composition, we consider in addition to the scenarios from fig. 1 also the possibility of a purely sterile initial flux, $(\Phi_{\nu_e} : \Phi_{\nu_\mu} : \Phi_{\nu_\tau} : \Phi_{\nu_s}) = (0 : 0 : 0 : 1)$. We show in color the parameter points corresponding to the 68% (left), 90% (middle) and 95% (right) credibility intervals from a global fit to short and long baseline data [47] (see text for details). The regions delineated by dashed black lines are the corresponding intervals without sterile neutrinos from fig. 1. Large solid black contours correspond to the IceCube constraint on the flavor ratios [69]. Once again, the results shown here are for normal neutrino mass ordering.

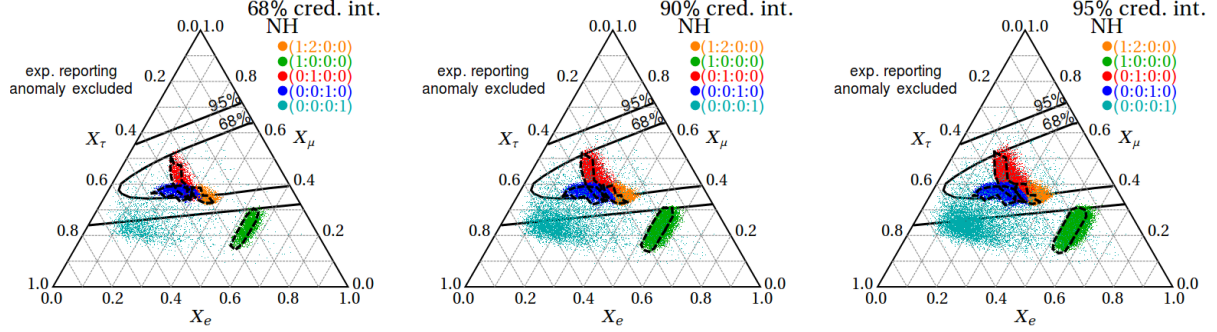


FIG. 3. Same as fig. 2, but excluding the anomalous data sets from LSND, MiniBooNE, short-baseline reactor experiments, and Gallium experiments in constraining the sterile neutrino mixing parameters.

credible interval obtained from the Bayesian global fit described in section II. By comparing to the credible intervals in the 3-flavor case (black dashed contours in fig. 2), we see that, for initial flavor compositions consisting only of active neutrinos, the situation is very similar to the standard scenario without sterile neutrinos. Large deviations from the 3-flavor situation are not possible given that active–sterile mixing angles are constrained to be $\lesssim \mathcal{O}(10\%)$ [47]. On the other hand, for flux components that are initially purely sterile (cyan regions in fig. 2), the observed flavor ratios at Earth are preferably in the lower left part of the flavor triangle, with relatively large ν_τ component and much smaller ν_e and ν_μ admixtures. This is also easily understandable: θ_{34} is much more weakly constrained than θ_{14} and θ_{24} , so that $P_{\nu_s \rightarrow \nu_\tau}$ can be large [47]. Comparing to IceCube constraints (black contours in fig. 2), we see that an initial neutrino flux consisting purely of ν_e (e.g. from neutron decay) is disfavored, as in the standard 3-flavor case. A purely sterile initial flux is still allowed, depending on the exact values of the mixing angles. Note, however, that IceCube constraints are based on the whole neutrino energy spectrum above ~ 10 TeV, and that an initial flux consisting only of ν_s throughout this energy range seems not very plausible theoretically.

For illustration, we have also investigated how the results shown in fig. 2 change when the short-baseline anomalies from LSND, MiniBooNE, short-baseline reactor experiments, and Gallium experiments are disregarded, see fig. 3. We see virtually no change compared to fig. 2, which indicates that the global fit is dominated by the null searches. The largest differences are observed for purely sterile initial flux, where the preferred flavor ratios at Earth are shifted towards pure ν_τ flavor when the anomalies are disregarded. The reason is that limits on θ_{14} and θ_{24} are more stringent in this case, while constraints on θ_{34} are not affected by the anomalous data sets.

Even though we have considered scenarios with initial flavor composition $(0 : 0 : 0 : 1)$ in figs. 2 and 3, we have emphasized that a purely sterile initial flux is not very likely, neither from a theoretical point of view nor from looking at the IceCube data. Therefore, we illustrate in fig. 4 how the predicted flavor fractions at Earth change as a function of the ν_s admixture to the initial flux. The two parameterizations for the initial flavor composition shown in this figure, $(\frac{1-x}{3} : \frac{2(1-x)}{3} : 0 : x)$ and $(0 : 1-x : 0 : x)$ correspond to an admixture of sterile neutrinos (e.g. from DM decay) to an astrophysical flux from pion decay, or from pion decay with strong muon energy loss (muon-damped source), respectively.

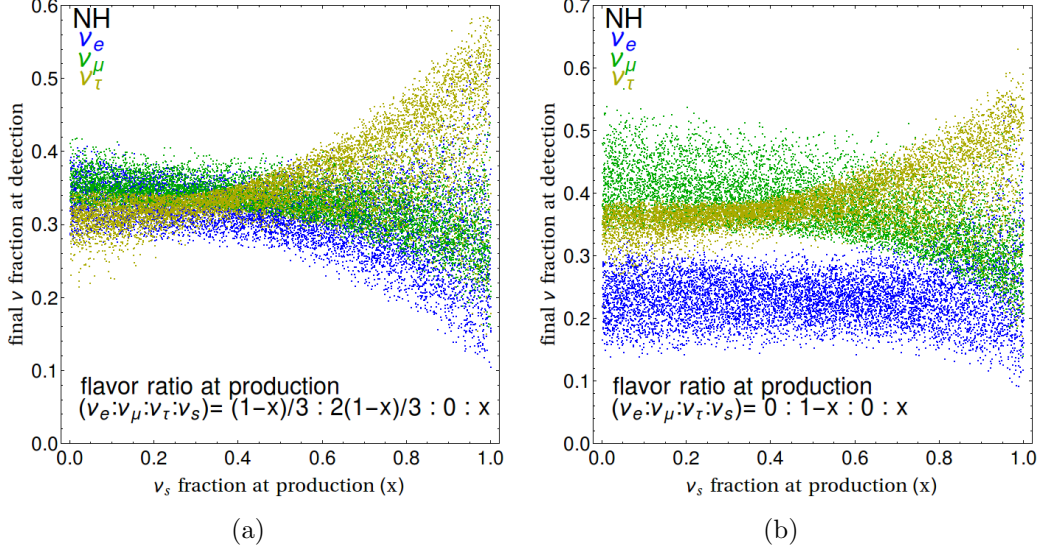


FIG. 4. The individual flavor fractions at Earth for varying initial ν_s admixture. In panel (a), we take the initial flavor ratios to be of the form $\Phi_{\nu_e} : \Phi_{\nu_\mu} : \Phi_{\nu_\tau} : \Phi_{\nu_s} = (\frac{1-x}{3} : \frac{2(1-x)}{3} : 0 : x)$, with $0 < x < 1$. An initial flavor composition of this form could arise, for instance, from an astrophysical flux from pion decay plus a ν_s flux from dark matter decay. In panel (b) we use the parameterization $(0 : 1-x : 0 : x)$ with $0 < x < 1$ for the initial flux, corresponding for instance to a muon-damped astrophysical source plus ν_s from DM decay. The parameter points shown in both panels correspond to the 95% credible interval.

IV. DARK MATTER DECAY AND FITS TO ICECUBE DATA

To illustrate how flavor ratios of high-energy neutrinos can be used to probe and discriminate between particle physics models, we discuss in the following two toy scenarios in which neutrinos are produced not only by conventional astrophysical sources, but also in the decay of PeV-scale DM particles. The two toy models of interest to us are:

- **Model 1: Heavy right-handed neutrino DM.**

In this scenario, the DM particles N are fermionic and are total singlets under the SM gauge group. They are allowed to decay to SM particles via the neutrino portal interactions

$$\mathcal{L}_{\text{int}} \supset \sum_{\alpha} y_{\alpha} \bar{N} \tilde{H}^{\dagger} L_{\alpha} + \text{h.c.} \quad (8)$$

Here, H is the SM Higgs boson, $\tilde{H} = i\sigma^2 H^*$, and L_{α} is the SM lepton doublet of flavor α . We assume that the couplings of N to first and second generation leptons are suppressed ($y_{\tau} \gg y_e, y_{\mu}$). With this assumption, the model predicts that in half of the N decays, a monoenergetic tau neutrino with initial spectrum $dN_{\nu}/dE_{\nu} = \delta(m_{\text{DM}}/2 - E_{\nu})$ is produced. Here, m_{DM} is the mass of the DM particle N . Note that the model also predicts a secondary neutrino flux at lower energies, coming from decays of the Higgs boson produced in association with the monoenergetic neutrinos, the decay products of the W bosons produced together with charged leptons, and from the decays of Z bosons. We compute all secondary neutrino fluxes using ref. [70] (with electroweak corrections based on ref. [71]) and cross-checked with those presented in [72, 73].

We require that y_{τ} is tiny, so that the lifetime of N [72],

$$\tau_{\text{DM}} = \frac{4\pi}{m_{\text{DM}} y_{\tau}^2} \quad (9)$$

is much larger than the age of the Universe and that gamma ray constraints are satisfied [73]. The N mass is taken to be $\mathcal{O}(\text{PeV})$. The smallness of y_τ could for instance be explained in scenarios with warped extra dimensions, where the wave function overlap between SM fields living on the infrared brane and N living on the ultraviolet brane can be minuscule.

- **Model 2: Scalar DM decaying to sterile neutrinos.** This model is based on the Yukawa interaction

$$\mathcal{L}_{\text{int}} \supset y_2 \phi \bar{\nu}_s \nu_s + \text{h.c.}, \quad (10)$$

where ϕ is the scalar DM particle with mass $m_{\text{DM}} \sim \mathcal{O}(\text{PeV})$ and ν_s is eV-scale sterile neutrino introduced in section II. We again assume the Yukawa coupling y_2 to be tiny so that the lifetime of ϕ ,

$$\tau_{\text{DM}} = \frac{4\pi}{m_{\text{DM}} y_2^2} \quad (11)$$

is much larger than the age of the Universe. The sterile neutrinos ν_s are assumed to mix with the active ones to lead to observable signals in IceCube.

In computing the expected neutrino fluxes at the detector, we need to distinguish between neutrinos from DM decay in the Milky Way and neutrino from DM decay in distant galaxies. The galactic component of the flux is not affected by redshift, while the energy spectrum of extragalactic neutrinos is smeared out towards lower energies because of contributions from high-redshift galaxies. The differential flux of galactic neutrinos from DM decay can be written as [74–79]

$$\frac{dJ_{\text{gal}}}{dE_\nu} \approx 1.7 \times 10^{-5} \text{ cm}^{-2} \text{ s}^{-1} \text{ sr}^{-1} \left(\frac{1 \text{ GeV}}{m_{\text{DM}}} \right) \left(\frac{10^{26} \text{ s}}{\tau_{\text{DM}}} \right) \times \frac{dN_\nu(E_\nu)}{dE_\nu}, \quad (12)$$

where $dN_\nu(E_\nu)/dE_\nu$ is the initial neutrino spectrum at production. For neutrinos from extragalactic DM decay, we have instead [75]

$$\frac{dJ_{\text{extragal}}}{dE_\nu} = \frac{\Omega_{\text{DM}} \rho_c}{4\pi m_{\text{DM}} \tau_{\text{DM}}} \int_0^\infty dz \frac{1}{H(z)} \frac{dN_\nu((1+z)E_\nu)}{dE_\nu} \quad (13)$$

$$\approx 1.4 \times 10^{-5} \text{ cm}^{-2} \text{ s}^{-1} \text{ sr}^{-1} \left(\frac{1 \text{ GeV}}{m_{\text{DM}}} \right) \left(\frac{10^{26} \text{ s}}{\tau_{\text{DM}}} \right) \times \int_0^{\frac{m_{\text{DM}}}{2E_\nu} - 1} dz \frac{1}{\sqrt{\Omega_\Lambda + \Omega_m(1+z)^3}} \frac{dN_\nu((1+z)E_\nu)}{dE_\nu}, \quad (14)$$

where Ω_{DM} , Ω_m , and Ω_Λ are the dark matter density, total matter density, and dark energy density of the Universe, respectively, all expressed in units of the critical density ρ_c . Moreover, z is the redshift, and E_ν is the neutrino energy at Earth, after redshifting. Note that we have assumed the Universe to be perfectly transparent to neutrinos, which is usually a safe assumption [75].

We will fit four-year high energy starting events (HESE) data from IceCube [33, 80] as well as two years of through-going muons (TGM) data [81]. Note that we do not make use of the more recent 6-year TGM analysis [82] which, unlike the 2-year one [81], is not accompanied by a full digital data release. In particular, the response tensor $A_{\text{eff}}(E_\mu, E_\nu)$, which relates the true neutrino energy E_ν to the reconstructed muon energy E_μ , is not available. For HESE data, we make the simplification of equating the true neutrino energy and the electromagnetic energy deposited in the detector.

The total number of DM-induced HESE events expected in IceCube in an energy interval $[E_a, E_b]$ is obtained as

$$N_{\text{DM}}(E_a < E_\nu < E_b) = \int_{E_a}^{E_b} dE_\nu \sum_{f=e,\bar{e},\mu,\bar{\mu},\tau,\bar{\tau}} \Delta\Omega \Delta t A_{\text{eff}}^f(E_\nu) \left(\frac{dJ_{\text{extragal}}^{f,\text{osc}}}{dE_\nu} + \frac{dJ_{\text{gal}}^{f,\text{osc}}}{dE_\nu} \right), \quad (15)$$

where Δt is the length of the data taking period, $A_{\text{eff}}(E_\nu)$ is the energy dependent effective area of the detector [32], and $\Delta\Omega$ is the solid angle range to which the experiment is sensitive. For high energy starting events, we have $\Delta\Omega = 4\pi$. The superscript “osc” in $dJ_{\text{extragal}}^{f,\text{osc}}/dE_\nu$ and $dJ_{\text{gal}}^{f,\text{osc}}/dE_\nu$ denotes that neutrino oscillations are taken into account in these fluxes (as opposed to eqs. (12) and (14), which give unoscillated fluxes). For model 1, we use the best fit oscillation parameter values from [67], while for model 2 we use the best fit parameter set from our sterile neutrino fits, based on [47].

Regarding TGM, the corresponding event number in i -th reconstructed muon energy bin can be expressed as

$$N(E_a < E_\mu < E_b) = \int_{E_a}^{E_b} dE_\mu \int dE_\nu \sum_{f=\mu,\bar{\mu},\tau,\bar{\tau}} \Delta\Omega \Delta t \frac{dA_{\text{eff}}^f(E_\mu, E_\nu)}{dE_\mu} \left(\frac{dJ_{\text{extragal}}^{f,\text{osc}}}{dE_\nu} + \frac{dJ_{\text{gal}}^{f,\text{osc}}}{dE_\nu} \right). \quad (16)$$

Here, the index f denotes the neutrino flavor at Earth. Note also that the response tensor $A_{\text{eff}}^f(E_\mu, E_\nu)$ (which here has been integrated over zenith angles) is different for data taken in 2010 and data taken in 2011. Therefore, we compute the two contributions separately, and then sum them. Note that $\Delta\Omega = 2\pi$ here since only upward going muons can be reliably distinguished from background. With only 2π of sky coverage, also the numerical prefactor in eq. (12) changes. Numerically, we obtain $1.28 \times 10^{-5} \text{ cm}^{-2} \text{ s}^{-1} \text{ sr}^{-1}$ for the TGM analysis.

For the primary spectrum of the astrophysical component of the neutrino flux, we consider a simple power law,

$$\frac{dN_{\nu,\text{astro}}}{dE_\nu} = J_0 \cdot \left(\frac{E_\nu}{100 \text{ TeV}} \right)^{-\gamma}, \quad (17)$$

with normalization J_0 (in units of $\text{GeV}^{-1} \text{ cm}^{-2} \text{ sec}^{-1} \text{ sr}^{-1}$) and power law index γ . For the astrophysical flux, we assume a flavor ratio of (1 : 1 : 1) at Earth, and we assume equal fluxes of neutrinos and antineutrinos. The total number of measured events from astrophysical sources is obtained in analogy to eqs. (15) and (16).

We use the log likelihood ratio (LLR) method to determine the parameters in our toy models. The LLR is defined as

$$\begin{aligned} & \text{LLR}(m_{\text{DM}}, \tau_{\text{DM}}, J_0, \gamma) \\ &= \log \left(\frac{\text{Max}_{x \in [-\infty, \infty]} \left[f_{\text{Gauss}}(x) \prod_i f_{\text{Poisson}}(S_i(m_{\text{DM}}, \tau_{\text{DM}}, J_0, \gamma) + B_i + x \Delta B_i | O_i) \right]}{\text{Max}_{x' \in [-\infty, \infty]} \left[f_{\text{Gauss}}(x') \prod_i f_{\text{Poisson}}(B_i + x' \Delta B_i | O_i) \right]} \right). \quad (18) \end{aligned}$$

Here, $f_{\text{Gauss}}(x)$ is a normal distribution in x , with zero mean and variance 1, and $f_{\text{Poisson}}(\mu|n) = \mu^n e^{-\mu}/n!$ is the Poisson likelihood function. $S_i(m_{\text{DM}}, \tau_{\text{DM}}, J_0, \gamma)$ is the predicted signal event rate in the i -th bin (including astrophysical and DM-induced contributions), B_i is the atmospheric background, and ΔB_i is its uncertainty. Finally, O_i are the observed event rates. We compute the log-likelihood ratios for both HESE and TGM data and sum them up:

$$\text{LLR}_{\text{total}}(m_{\text{DM}}, \tau_{\text{DM}}, J_0, \gamma) = \text{LLR}_{\text{HESE}}(m_{\text{DM}}, \tau_{\text{DM}}, J_0, \gamma) + \text{LLR}_{\text{TGM}}(m_{\text{DM}}, \tau_{\text{DM}}, J_0, \gamma). \quad (19)$$

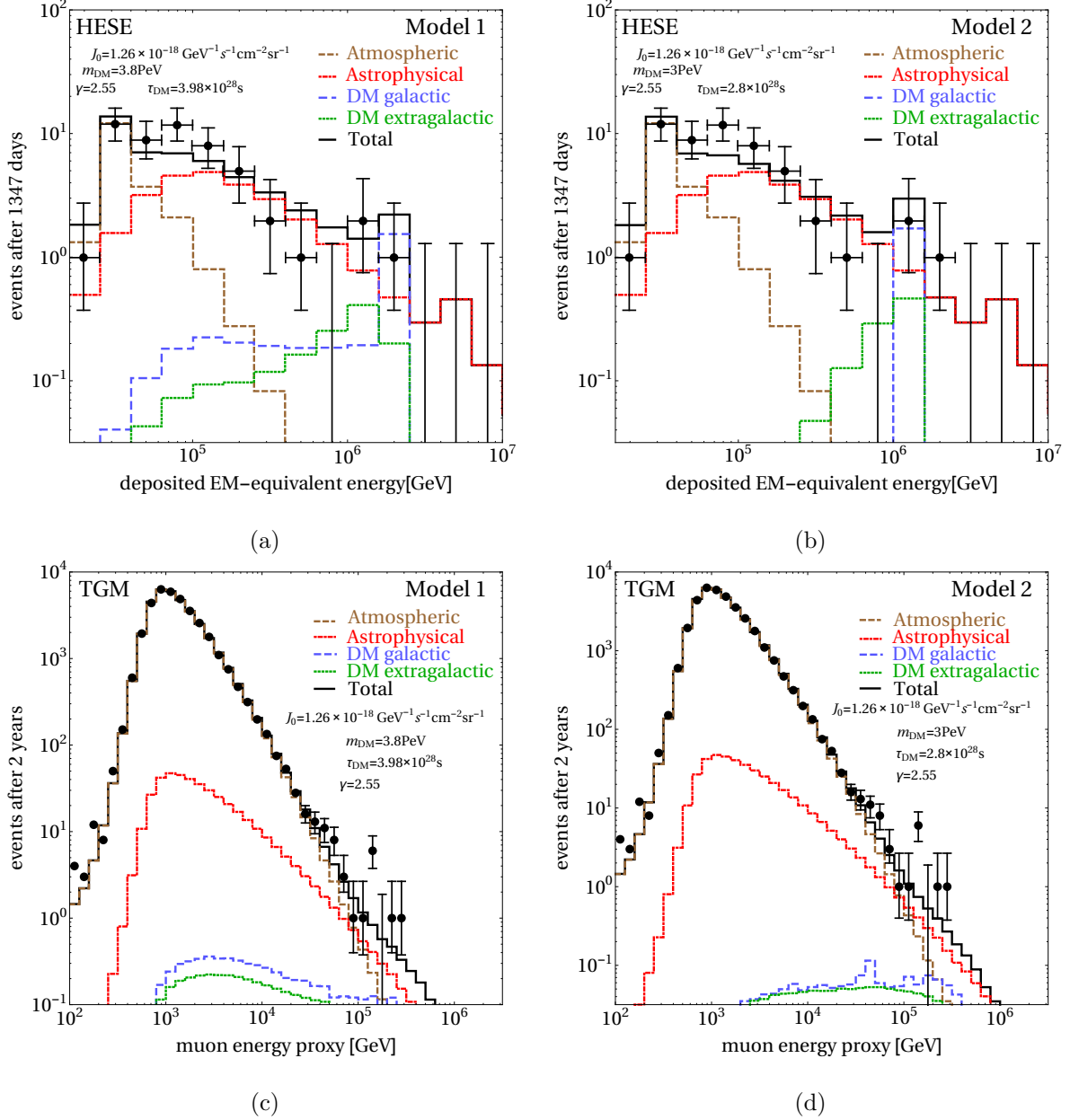


FIG. 5. Predicted neutrino fluxes in model 1 (left) and model 2 (right), compared to four-year HESE (high energy starting event) data [33, 80] (top) and two-year TGM (through-going muon data) [81]. The model parameters (indicated in the plots) are given by the best fit point of a combined fit to HESE and TGM data.

The results of our fit are shown in figs. 5 and 6. In fig. 5 we compare the predicted signal and background fluxes at the respective best fit points for model 1 and model 2 to IceCube data. Overall, we find an excellent fit, showing that the IceCube data admits (and in fact prefers) an admixture of neutrinos from DM decay to the astrophysical neutrino flux. This is also evident from fig. 6, where we explore the preferred parameter regions in more detail. We see that the fit, which is driven by the HESE data, prefers DM masses around a few PeV. In this case, the HESE events above 1 PeV could be explained as coming from DM decay, while the lower energy excess events would be explained by astrophysical sources. Note that the astrophysical power law index

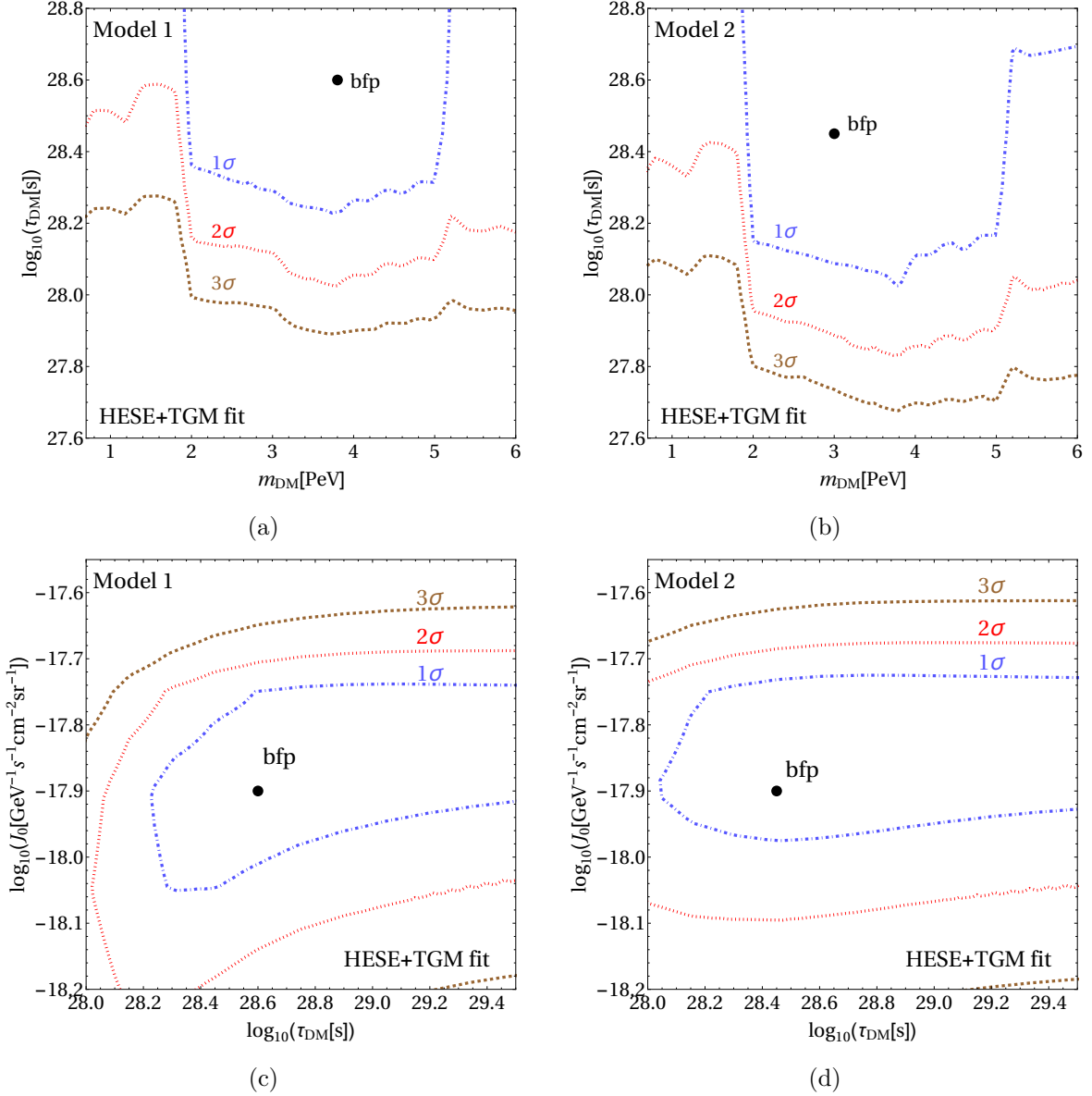


FIG. 6. Results from combined fits to HESE and TGM data. Panels (a) and (c) correspond to model 1, while panels (b) and (d) are for model 2. In the upper panels, (a) and (b), we show the best fit point (bfp) and the 1, 2, 3 σ preferred regions contours in the plane spanned by the dark matter mass m_{DM} and its lifetime τ_{DM} . In the bottom panel, we plot τ_{DM} vs. the normalization of the astrophysical flux, J_0 . In each plot, we project over the parameters not shown.

γ required to fit the data is fairly independent of the DM parameters, hence we do not show it explicitly in fig. 6.

Note that the log-likelihood ratio at the best fit point of model 2 is 50, with the contribution from HESE data being 35 and that from TGM data 15. A HESE-only fit yields a LLR of 38 at its best fit point, and a TGM-only fit yields 19. The fact that the sum of the last two numbers, 57, is larger than the LLR at the combined best fit, indicates some tension between the TGM and HESE data sets when interpreted in terms of astrophysical neutrinos plus a contribution from DM decay. This tension is mostly driven by the astrophysical component of the flux, and was found also by the IceCube collaboration in studies where a neutrino flux from DM decay was not considered [69, 82].

V. SUMMARY AND CONCLUSIONS

In summary, we have explored the possible impact of light sterile neutrinos on the flavor ratios of astrophysical neutrinos, measured by neutrino telescopes. We have seen that the accessible regions in the flavor triangle are enlarged, though not dramatically. The reason are the relatively stringent experimental constraints on active–sterile neutrino mixing, which we take into account by running a full global fit to short and long baseline data.

We have then discussed the interesting possibility that the initial flux of astrophysical neutrinos at production is purely sterile. While this is probably not true across the energy spectrum, it can happen in a limited energy window, namely, in scenarios where dark matter decays predominantly to sterile neutrinos and dominates the neutrino flux in some energy range. In this case, the flavor ratios at Earth can be very different from those in the 3-flavor case. The accessible region in the flavor triangle is then shifted towards pure tau flavor, as constraints on ν_τ – ν_s mixing are weakest.

To illustrate what it takes to obtain an unusual initial flavor composition, we have carried out in the second part of the paper a fit to IceCube data in two dark matter toy models: (1) decay of total singlet DM, N , via an operator of the form $\bar{L}HN$, which can lead to a primary flux dominated by ν_τ at $E_\nu \sim m_{\text{DM}}/2$. (2) decay of scalar DM to sterile neutrinos. We have considered high energy starting events (HESE) and through-going muon (TGM) data. As flavor ratios do not have serious model discrimination power yet, we have only fitted the energy spectra. In both toy models, we have found excellent fits to the data, and we have explored the viable parameter space. This highlights that the two toy models we consider could be possible targets for future analyses of IceCube or IceCube Gen-2 data, which could then also take into account the flavor composition as a function of energy.

ACKNOWLEDGMENTS

We would like to thank Carlos Argüelles, Pilar Coloma, Mona Dentler, and Jia Liu for very useful and interesting discussions. JK’s work was in part carried out at Fermilab and at the Aspen Center for Physics (NSF grant PHY-1066293), while VB was visiting the Wisconsin IceCube Particle Astrophysics Center during the final stages of this project. It is a pleasure to thank these institutions for their hospitality and support. This work has been supported by the German Research Foundation (DFG) under Grant Nos. KO 4820/1–1, FOR 2239, EXC-1098 (PRISMA) and by the European Research Council (ERC) under the European Union’s Horizon 2020 research and innovation programme (grant agreement No. 637506, “ ν Directions”).

-
- [1] **Virgo, LIGO Scientific Collaboration**, B. P. Abbott *et al.*, *Observation of Gravitational Waves from a Binary Black Hole Merger*, *Phys. Rev. Lett.* **116** (2016), no. 6 061102, [[1602.03837](#)].
 - [2] G. Barenboim and C. Quigg, *Neutrino observatories can characterize cosmic sources and neutrino properties*, *Phys. Rev.* **D67** (2003) 073024, [[hep-ph/0301220](#)].
 - [3] M. Cirelli, G. Marandella, A. Strumia, and F. Vissani, *Probing oscillations into sterile neutrinos with cosmology, astrophysics and experiments*, *Nucl.Phys.* **B708** (2005) 215–267, [[hep-ph/0403158](#)].
 - [4] Z.-Z. Xing and S. Zhou, *Towards determination of the initial flavor composition of ultrahigh-energy neutrino fluxes with neutrino telescopes*, *Phys. Rev.* **D74** (2006) 013010, [[astro-ph/0603781](#)].
 - [5] P. Lipari, M. Lusignoli, and D. Meloni, *Flavor Composition and Energy Spectrum of Astrophysical Neutrinos*, *Phys. Rev.* **D75** (2007) 123005, [[0704.0718](#)].
 - [6] S. Pakvasa, W. Rodejohann, and T. J. Weiler, *Flavor Ratios of Astrophysical Neutrinos: Implications for Precision Measurements*, *JHEP* **02** (2008) 005, [[0711.4517](#)].

- [7] M. Blennow and D. Meloni, *Non-standard interaction effects on astrophysical neutrino fluxes*, *Phys.Rev.* **D80** (2009) 065009, [[arXiv:0901.2110](#)].
- [8] A. Esmaili and Y. Farzan, *An Analysis of Cosmic Neutrinos: Flavor Composition at Source and Neutrino Mixing Parameters*, *Nucl. Phys.* **B821** (2009) 197–214, [[0905.0259](#)].
- [9] K.-C. Lai, G.-L. Lin, and T. C. Liu, *Determination of the Neutrino Flavor Ratio at the Astrophysical Source*, *Phys. Rev.* **D80** (2009) 103005, [[0905.4003](#)].
- [10] S. Choubey and W. Rodejohann, *Flavor Composition of UHE Neutrinos at Source and at Neutrino Telescopes*, *Phys. Rev.* **D80** (2009) 113006, [[0909.1219](#)].
- [11] A. Bhattacharya, S. Choubey, R. Gandhi, and A. Watanabe, *Ultra-high neutrino fluxes as a probe for non-standard physics*, *JCAP* **1009** (2010) 009, [[1006.3082](#)].
- [12] D. Hollander, *Astrophysical neutrino flavor ratios in the presence of sterile neutrinos*, [1301.5313](#).
- [13] P. Keranen, J. Maalampi, M. Myrskylainen, and J. Riittinen, *Effects of sterile neutrinos on the ultrahigh-energy cosmic neutrino flux*, *Phys. Lett.* **B574** (2003) 162–168, [[hep-ph/0307041](#)].
- [14] S. Rajpoot, S. Sahu, and H. C. Wang, *Detection of ultra high energy neutrinos by IceCube: Sterile neutrino scenario*, *Eur. Phys. J.* **C74** (2014), no. 6 2936, [[1310.7075](#)].
- [15] O. Mena, S. Palomares-Ruiz, and A. C. Vincent, *Flavor Composition of the High-Energy Neutrino Events in IceCube*, *Phys. Rev. Lett.* **113** (2014) 091103, [[1404.0017](#)].
- [16] X.-J. Xu, H.-J. He, and W. Rodejohann, *Constraining Astrophysical Neutrino Flavor Composition from Leptonic Unitarity*, *JCAP* **1412** (2014) 039, [[1407.3736](#)].
- [17] L. Fu, C. M. Ho, and T. J. Weiler, *Aspects of the Flavor Triangle for Cosmic Neutrino Propagation*, *Phys. Rev.* **D91** (2015) 053001, [[1411.1174](#)].
- [18] S. Palomares-Ruiz, A. C. Vincent, and O. Mena, *Spectral analysis of the high-energy IceCube neutrinos*, *Phys. Rev.* **D91** (2015), no. 10 103008, [[1502.02649](#)].
- [19] A. Palladino, G. Pagliaroli, F. L. Villante, and F. Vissani, *What is the Flavor of the Cosmic Neutrinos Seen by IceCube?*, *Phys. Rev. Lett.* **114** (2015), no. 17 171101, [[1502.02923](#)].
- [20] **IceCube Collaboration**, M. G. Aartsen *et al.*, *Flavor Ratio of Astrophysical Neutrinos above 35 TeV in IceCube*, *Phys. Rev. Lett.* **114** (2015), no. 17 171102, [[1502.03376](#)].
- [21] N. Kawanaka and K. Ioka, *Neutrino Flavor Ratios Modified by Cosmic Ray Secondary Acceleration*, *Phys. Rev.* **D92** (2015), no. 8 085047, [[1504.03417](#)].
- [22] A. Palladino and F. Vissani, *The natural parameterization of cosmic neutrino oscillations*, *Eur. Phys. J.* **C75** (2015) 433, [[1504.05238](#)].
- [23] C. A. Argelles, T. Katori, and J. Salvado, *New Physics in Astrophysical Neutrino Flavor*, *Phys. Rev. Lett.* **115** (2015) 161303, [[1506.02043](#)].
- [24] M. Bustamante, J. F. Beacom, and W. Winter, *Theoretically palatable flavor combinations of astrophysical neutrinos*, *Phys. Rev. Lett.* **115** (2015), no. 16 161302, [[1506.02645](#)].
- [25] **IceCube Collaboration**, M. G. Aartsen *et al.*, *A combined maximum-likelihood analysis of the high-energy astrophysical neutrino flux measured with IceCube*, [1507.03991](#).
- [26] M. C. Gonzalez-Garcia, M. Maltoni, I. Martinez-Soler, and N. Song, *Non-standard neutrino interactions in the Earth and the flavor of astrophysical neutrinos*, *Astropart. Phys.* **84** (2016) 15–22, [[1605.08055](#)].
- [27] S. W. Li, M. Bustamante, and J. F. Beacom, *Echo Technique to Distinguish Flavors of Astrophysical Neutrinos*, [1606.06290](#).
- [28] I. M. Shoemaker and K. Murase, *Probing BSM Neutrino Physics with Flavor and Spectral Distortions: Prospects for Future High-Energy Neutrino Telescopes*, *Phys. Rev.* **D93** (2016), no. 8 085004, [[1512.07228](#)].
- [29] A. Chatterjee, M. M. Devi, M. Ghosh, R. Moharana, and S. K. Raut, *Probing CP violation with the first three years of ultrahigh energy neutrinos from IceCube*, *Phys. Rev.* **D90** (2014), no. 7 073003, [[1312.6593](#)].
- [30] C.-Y. Chen, P. S. Bhupal Dev, and A. Soni, *Two-component flux explanation for the high energy neutrino events at IceCube*, *Phys. Rev.* **D92** (2015), no. 7 073001, [[1411.5658](#)].
- [31] H. Nunokawa, B. Panes, and R. Zukanovich Funchal, *How Unequal Fluxes of High Energy Astrophysical Neutrinos and Antineutrinos can Fake New Physics*, *JCAP* **1610** (2016), no. 10 036, [[1604.08595](#)].
- [32] **IceCube Collaboration**, M. G. Aartsen *et al.*, *Evidence for High-Energy Extraterrestrial Neutrinos at the IceCube Detector*, *Science* **342** (2013) 1242856, [[1311.5238](#)].

- [33] **IceCube Collaboration**, M. G. Aartsen *et al.*, *Observation of High-Energy Astrophysical Neutrinos in Three Years of IceCube Data*, *Phys. Rev. Lett.* **113** (2014) 101101, [[1405.5303](#)].
- [34] **LSND Collaboration**, A. Aguilar *et al.*, *Evidence for neutrino oscillations from the observation of $\bar{\nu}_e$ appearance in a $\bar{\nu}_\mu$ beam*, *Phys. Rev.* **D64** (2001) 112007, [[hep-ex/0104049](#)].
- [35] **MiniBooNE Collaboration**, A. Aguilar-Arevalo *et al.*, *Improved Search for $\bar{\nu}_\mu \rightarrow \bar{\nu}_e$ Oscillations in the MiniBooNE Experiment*, *Phys.Rev.Lett.* **110** (2013) 161801, [[1207.4809](#)].
- [36] M. A. Acero, C. Giunti, and M. Laveder, *Limits on $\nu(e)$ and anti- $\nu(e)$ disappearance from Gallium and reactor experiments*, *Phys.Rev.* **D78** (2008) 073009, [[0711.4222](#)].
- [37] C. Giunti and M. Laveder, *Statistical Significance of the Gallium Anomaly*, *Phys.Rev.* **C83** (2011) 065504, [[1006.3244](#)].
- [38] T. Mueller, D. Lhuillier, M. Fallot, A. Letourneau, S. Cormon, *et al.*, *Improved Predictions of Reactor Antineutrino Spectra*, *Phys.Rev.* **C83** (2011) 054615, [[1101.2663](#)].
- [39] G. Mention, M. Fechner, T. Lasserre, T. Mueller, D. Lhuillier, *et al.*, *The Reactor Antineutrino Anomaly*, *Phys.Rev.* **D83** (2011) 073006, [[1101.2755](#)].
- [40] P. Huber, *On the determination of anti-neutrino spectra from nuclear reactors*, *Phys.Rev.* **C84** (2011) 024617, [[1106.0687](#)].
- [41] A. C. Hayes, J. L. Friar, G. T. Garvey, G. Jungman, and G. Jonkmans, *Systematic Uncertainties in the Analysis of the Reactor Neutrino Anomaly*, *Phys. Rev. Lett.* **112** (2014) 202501, [[1309.4146](#)].
- [42] D.-L. Fang and B. A. Brown, *Effect of first forbidden decays on the shape of neutrino spectra*, *Phys. Rev.* **C91** (2015), no. 2 025503, [[1502.02246](#)]. [Erratum: *Phys. Rev.*C93,no.4,049903(2016)].
- [43] A. C. Hayes and P. Vogel, *Reactor Neutrino Spectra*, [1605.02047](#).
- [44] J. Kopp, M. Maltoni, and T. Schwetz, *Are there sterile neutrinos at the eV scale?*, *Phys.Rev.Lett.* **107** (2011) 091801, [[1103.4570](#)].
- [45] J. Conrad, C. Ignarra, G. Karagiorgi, M. Shaevitz, and J. Spitz, *Sterile Neutrino Fits to Short Baseline Neutrino Oscillation Measurements*, *Adv.High Energy Phys.* **2013** (2013) 163897, [[1207.4765](#)].
- [46] M. Archidiacono, N. Fornengo, C. Giunti, S. Hannestad, and A. Melchiorri, *Sterile neutrinos: Cosmology versus short-baseline experiments*, *Phys. Rev.* **D87** (2013), no. 12 125034, [[1302.6720](#)].
- [47] J. Kopp, P. A. N. Machado, M. Maltoni, and T. Schwetz, *Sterile Neutrino Oscillations: The Global Picture*, *JHEP* **1305** (2013) 050, [[1303.3011](#)].
- [48] A. Mirizzi, G. Mangano, N. Saviano, E. Borriello, C. Giunti, *et al.*, *The strongest bounds on active-sterile neutrino mixing after Planck data*, [1303.5368](#).
- [49] C. Giunti, M. Laveder, Y. Li, and H. Long, *Pragmatic View of Short-Baseline Neutrino Oscillations*, *Phys.Rev.* **D88** (2013) 073008, [[1308.5288](#)].
- [50] S. Gariazzo, C. Giunti, and M. Laveder, *Light Sterile Neutrinos in Cosmology and Short-Baseline Oscillation Experiments*, *JHEP* **1311** (2013) 211, [[1309.3192](#)].
- [51] G. H. Collin, C. A. Argelles, J. M. Conrad, and M. H. Shaevitz, *Sterile Neutrino Fits to Short Baseline Data*, *Nucl. Phys.* **B908** (2016) 354–365, [[1602.00671](#)].
- [52] K. N. Abazajian *et al.*, *Light Sterile Neutrinos: A White Paper*, [1204.5379](#).
- [53] J. Hasenkamp, *Neutrino self-interactions*, *Phys. Rev.* **D93** (2016), no. 5 055033, [[1604.04742](#)].
- [54] J. F. Cherry, A. Friedland, and I. M. Shoemaker, *Short-baseline neutrino oscillations, Planck, and IceCube*, [1605.06506](#).
- [55] T. Kashti and E. Waxman, *Flavoring astrophysical neutrinos: Flavor ratios depend on energy*, *Phys. Rev. Lett.* **95** (2005) 181101, [[astro-ph/0507599](#)].
- [56] W. Winter, *Describing the Observed Cosmic Neutrinos by Interactions of Nuclei with Matter*, *Phys. Rev.* **D90** (2014), no. 10 103003, [[1407.7536](#)].
- [57] E. Waxman and J. N. Bahcall, *High-energy neutrinos from cosmological gamma-ray burst fireballs*, *Phys. Rev. Lett.* **78** (1997) 2292–2295, [[astro-ph/9701231](#)].
- [58] J. P. Rachen and P. Meszaros, *Photohadronic neutrinos from transients in astrophysical sources*, *Phys. Rev.* **D58** (1998) 123005, [[astro-ph/9802280](#)].
- [59] S. I. Blinnikov, *Notes on Hidden Mirror World*, *Phys. Atom. Nucl.* **73** (2010) 593–603, [[0904.3609](#)].
- [60] R. Foot, *Mirror dark matter: Cosmology, galaxy structure and direct detection*, *Int. J. Mod. Phys.* **A29** (2014) 1430013, [[1401.3965](#)].
- [61] C. Giunti and C. W. Kim, *Fundamentals of Neutrino Physics and Astrophysics*. Oxford University Press, 2007.

- [62] A. de Gouvea and J. Jenkins, *The Physical Range of Majorana Neutrino Mixing Parameters*, *Phys.Rev.* **D78** (2008) 053003, [[0804.3627](#)].
- [63] N. Haba and H. Murayama, *Anarchy and hierarchy*, *Phys. Rev.* **D63** (2001) 053010, [[hep-ph/0009174](#)].
- [64] C. Spengler, M. Huber, and B. C. Hiesmayr, *Composite parameterization and Haar measure for all unitary and special unitary groups*, *Journal of Mathematical Physics* **53** (Jan., 2012) 013501–013501, [[1103.3408](#)].
- [65] V. Brdar, M. Knig, and J. Kopp, *Neutrino Anarchy and Renormalization Group Evolution*, *Phys. Rev.* **D93** (2016), no. 9 093010, [[1511.06371](#)].
- [66] M. Kendall, A. Stuart, and J. Ord, *Vol. 1: Distribution theory*. London [etc.]: Arnold [etc.], 1994.
- [67] M. C. Gonzalez-Garcia, M. Maltoni, and T. Schwetz, *Updated fit to three neutrino mixing: status of leptonic CP violation*, *JHEP* **11** (2014) 052, [[1409.5439](#)].
- [68] I. Esteban, M. C. Gonzalez-Garcia, M. Maltoni, I. Martinez-Soler, and T. Schwetz, *Updated fit to three neutrino mixing: exploring the accelerator-reactor complementarity*, [1611.01514](#).
- [69] **IceCube Collaboration**, M. G. Aartsen *et al.*, *A combined maximum-likelihood analysis of the high-energy astrophysical neutrino flux measured with IceCube*, *Astrophys. J.* **809** (2015), no. 1 98, [[1507.03991](#)].
- [70] M. Cirelli, G. Corcella, A. Hektor, G. Hutsi, M. Kadastik, P. Panci, M. Raidal, F. Sala, and A. Strumia, *PPPC 4 DM ID: A Poor Particle Physicist Cookbook for Dark Matter Indirect Detection*, *JCAP* **1103** (2011) 051, [[1012.4515](#)]. [Erratum: *JCAP*1210,E01(2012)].
- [71] P. Ciafaloni, D. Comelli, A. Riotto, F. Sala, A. Strumia, and A. Urbano, *Weak Corrections are Relevant for Dark Matter Indirect Detection*, *JCAP* **1103** (2011) 019, [[1009.0224](#)].
- [72] T. Higaki, R. Kitano, and R. Sato, *Neutrino Universe*, *JHEP* **07** (2014) 044, [[1405.0013](#)].
- [73] A. Esmaili, S. K. Kang, and P. D. Serpico, *IceCube events and decaying dark matter: hints and constraints*, *JCAP* **1412** (2014), no. 12 054, [[1410.5979](#)].
- [74] Y. Bai, R. Lu, and J. Salvado, *Geometric Compatibility of IceCube TeV-PeV Neutrino Excess and its Galactic Dark Matter Origin*, *JHEP* **01** (2016) 161, [[1311.5864](#)].
- [75] A. Esmaili, A. Ibarra, and O. L. G. Peres, *Probing the stability of superheavy dark matter particles with high-energy neutrinos*, *JCAP* **1211** (2012) 034, [[1205.5281](#)].
- [76] K. Murase and J. F. Beacom, *Constraining Very Heavy Dark Matter Using Diffuse Backgrounds of Neutrinos and Cascaded Gamma Rays*, *JCAP* **1210** (2012) 043, [[1206.2595](#)].
- [77] P. S. B. Dev, D. Kazanas, R. N. Mohapatra, V. L. Teplitz, and Y. Zhang, *Heavy right-handed neutrino dark matter and PeV neutrinos at IceCube*, *JCAP* **1608** (2016), no. 08 034, [[1606.04517](#)].
- [78] C. S. Fong, H. Minakata, B. Panes, and R. Zukanovich Funchal, *Possible Interpretations of IceCube High-Energy Neutrino Events*, *JHEP* **02** (2015) 189, [[1411.5318](#)].
- [79] T. Cohen, K. Murase, N. L. Rodd, B. R. Safdi, and Y. Soreq, *Gamma-ray Constraints on Decaying Dark Matter and Implications for IceCube*, [1612.05638](#).
- [80] **IceCube Collaboration**, M. G. Aartsen *et al.*, *The IceCube Neutrino Observatory - Contributions to ICRC 2015 Part II: Atmospheric and Astrophysical Diffuse Neutrino Searches of All Flavors*, in *Proceedings, 34th International Cosmic Ray Conference (ICRC 2015): The Hague, The Netherlands, July 30-August 6, 2015*, 2015. [1510.05223](#).
- [81] **IceCube Collaboration**, M. G. Aartsen *et al.*, *Evidence for Astrophysical Muon Neutrinos from the Northern Sky with IceCube*, *Phys. Rev. Lett.* **115** (2015), no. 8 081102, [[1507.04005](#)]. data available from https://icecube.wisc.edu/science/data/HE_NuMu_diffuse.
- [82] **IceCube Collaboration**, M. G. Aartsen *et al.*, *Observation and Characterization of a Cosmic Muon Neutrino Flux from the Northern Hemisphere using six years of IceCube data*, [1607.08006](#).